

Reversible and irreversible magnetization in the high- T_c superconductor $Tl_2Ca_2Ba_2Cu_3O_{10}$

Y. Wolfus and Y. Yeshurun

Department of Physics, Bar-Ilan University, Ramat-Gan 52100, Israel

I. Felner

Racah Institute of Physics, The Hebrew University of Jerusalem, Jerusalem 91904, Israel

(Received 25 January 1989)

dc magnetic measurements on the high-temperature superconductor $Tl_2Ca_2Ba_2Cu_3O_{10}$ ($T_c = 113$ K), are reported. The zero-field-cooled and field-cooled magnetization curves coincide above a temperature T_{irr} which scales with the applied field as $H^{1/3}$. The magnetization curves in the irreversible region scales; the scaling field is a simple function of geometrical factors and critical currents. The magnetization above T_c is not linear with the field, suggesting magnetic correlations in the CuO_2 layers in the normal state.

I. INTRODUCTION

Superconducting oxides such as Tl-Cu-Ba-Cu-O exhibit a variety of interesting features which depend on their composition.^{1,2} Electrical resistivity and magnetization studies of polycrystalline samples of $Tl_2Ca_2Ba_2Cu_3O_{10}$ (2:2:2:3) have already been published;^{3,4} however, to the best of our knowledge, little work has been reported to date on the reversibility and irreversibility properties of these systems. From a technical standpoint, these properties have great significance in high- T_c compounds. The temperature, T_{irr} , which is defined as the temperature which separates reversible and irreversible regions, is magnetic-field dependent and scales with the applied field as H^n . The exponent n varies considerably in high- T_c systems.⁵⁻⁸

In the present paper we present a detailed study of the reversible and irreversible properties of the new 2:2:2:3 system with $T_c = 113$ K. We find in general that the qualitative magnetic behavior of this system is very similar to that found in other high- T_c superconductors.⁵⁻⁸ The irreversibility line is pushed to relatively low temperatures compared to, for example, Y-Ba-Cu-O.⁸ An interesting and intriguing feature of the present data is that all magnetization curves scale below T_{irr} . The Meissner fraction, that is, the field-cooled moment normalized by $-1/4\pi$, depends strongly on the field applied during the experiment.⁹ Even in the low-field limit its value is relatively small compared to other high- T_c systems, which means that most of the flux is trapped during the cooling procedure. Above T_c the magnetic moment is not linear with the applied field; the nature of this behavior will be discussed.

II. EXPERIMENTAL DETAILS

The sample of nominal composition $Tl_2Ca_2Ba_2Cu_3O_{10}$ (2:2:2:3 phase) was prepared by thoroughly mixing and grinding appropriate amounts of Tl_2O_3 , BaO_2 , CaO , and CuO , pressed into a pellet and put into an alumina crucible in an oven preheated to $890^\circ C$. There it was reacted for 10 min in flowing oxygen and then furnace cooled to

room temperature. X-ray-powder diffractometry revealed the presence of two phases, the majority phase (more than 90%, the 2:2:2:3 phase) and the minority phase (less than 10%) $Tl_2CaBa_2Cu_2O_8$ (2:1:2:2 phase). The lattice parameters for the 2:2:2:3 phase are $a = 3.827(2)$ Å and $c = 36.18(2)$ Å in complete agreement with Ref. 2. The dc susceptibility measurements on a solid ceramic piece were carried out in a commercial SHE SQUID magnetometer in various fields $3.5 \text{ Oe} < H < 40$ kOe as a function of temperature in the range of 5–180 K. The magnetization was measured by two different procedures: (a) The sample was zero-field cooled (ZFC) to 5 K, a field H was applied, and the magnetization of the shielding branch was measured as a function of temperature. (b) The sample was field cooled (FC) from above T_c in a field H and the Meissner branch was measured.

From magnetic measurements we have clear indications that the state of our Tl material is metastable on a time scale of months at room temperature. It is also possible that low-temperature thermal cycling during the various measurements affects the composition stability. The measurements reported here have been performed on a fresh sample (within one week of preparation).

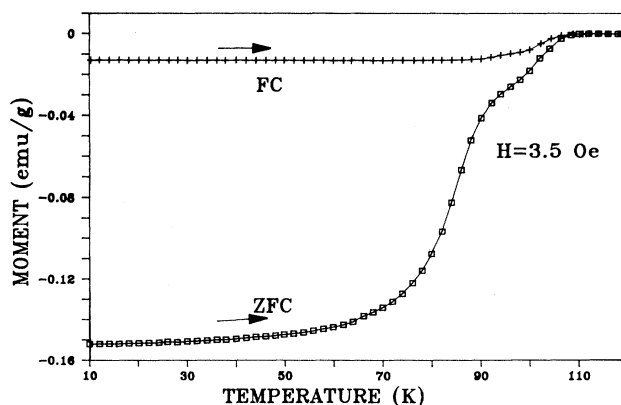


FIG. 1. ZFC and FC magnetic moment at 3.5 Oe for the 2:2:2:3 phase.

III. EXPERIMENTAL RESULTS AND DISCUSSION

The ZFC and FC magnetic curves for ceramic 2:2:2:3 phase measured at 3.5(5) Oe are shown in Fig. 1. The onset of T_c deduced from these curves is 113 K, in good agreement to 114 K obtained in single crystal with the same composition.¹⁰ For this relatively low field, there is no coincidence region between the curves in the neighborhood of T_c . The shielding (ZFC) diamagnetic value after sample demagnetization correction approaches 96% of $-1/4\pi$, and the volume Meissner fraction is only 8% of the ZFC value. This means that even in a field as low as this the flux expulsion is very incomplete and most of the magnetic flux is trapped and pinned during the cooling process.

A. The ZFC branch

In the ZFC branch of Fig. 1 a sharp decrease in the diamagnetic moment is observed at around 77 K. At 90 K a second step is observed and the rate of decrease is reduced until diamagnetism disappears at T_c . We denote the first temperature as T_{c1} and the second as T^* (Fig. 2). It might be thought that these two temperatures would be associated with superconducting transitions, 113 and 95 K, the two phases existing in the sample. However the small amount (less than 10%) of the 2:2:1:2 phase cannot explain the relatively large step (70%) in the magnetization between 77 and 90 K.

Following Krusin-Elbaum *et al.*,¹¹ who observed similar behavior in Y-Ba-Cu-O single crystals, we suggest that T_{c1} is the first temperature where the applied field equals H_{c1} and flux easily penetrates the sample. T^* is the temperature at which the external field penetrates the entire bulk for the first time.

Figure 2 exhibits M/H ZFC curves for several low applied fields. It is obvious that both T_{c1} and T^* shift systematically to lower temperatures with increasing H . T_{c1} is 68 and 62 K, and T^* is 86 and 82 K, for $H=10$ and 25 Oe, respectively. At higher fields the curve is too smeared to allow reasonable determination of T_{c1} and T^* . It is apparent from Fig. 2 that even in the low-field and low-

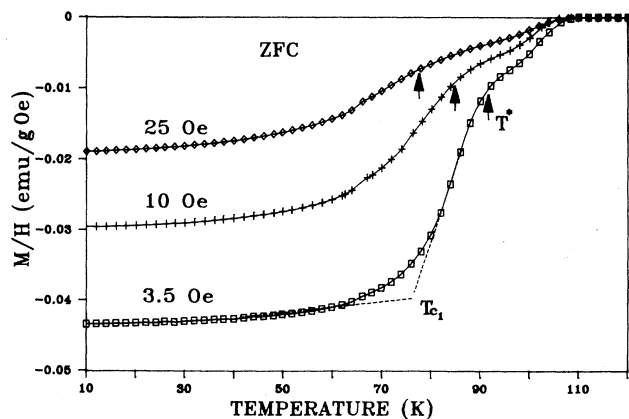


FIG. 2. ZFC magnetic-susceptibility curves at different magnetic fields. Note the shift to lower temperatures of T_{c1} and T^* .

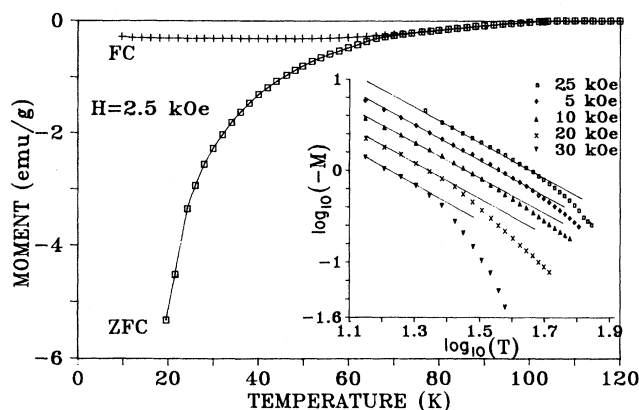


FIG. 3. ZFC and FC magnetization at 2.5 kOe. The inset shows the linear relation between M_{ZFC} and T^{-2} .

temperature limit, M is not linear with H . Two sources contribute to H_{c1} ,¹² the grains and the bulk. We attribute this deviation from linearity to flux penetration due to weak intergranular links. In other words, the "granular" H_{c1}^g value is lower than 10 Oe. The bulk H_{c1}^b value averaged over all crystallographic directions is deduced from the variation of T_{c1} . Assuming the regular parabolic dependence of H_c^1 with the reduced temperature, we estimate H_{c1}^b to be on the order of 50 Oe at low temperatures.

Figure 3 exhibits typical ZFC-FC curves in an applied magnetic field in the kOe region. In this field range the ZFC curves behave in quite a different manner. For a wide range of temperatures the magnetization is proportional to $T^{-2 \pm 0.1}$. This is demonstrated in the inset of Fig. 3 which shows several ZFC curve fits on a log-log scale for various fields between 2.5 and 30 kOe.

To explain this intriguing behavior we use the expression for the ZFC magnetization, M_{ZFC} , given in Ref. 11 where an extended Bean model¹³ yields two additive contributions to M_{ZFC} : from H_{c1} and from J_c . The relative weight of each term depends on the details of the temperature dependence of H_{c1} and J_c .¹¹ It is expected that at high fields ($H \gg H_{c1}$) the main contribution to M_{ZFC} comes from J_c . Thus, the inset of Fig. 3 suggests that $J_c \propto T^{-2}$. At higher temperatures a deviation from linearity is observed, since $J_c(H)$ is very small and no longer dominates the temperature dependence.

B. The FC branch

Figure 4 exhibits FC curves for various high external fields. The most striking feature is the upward turn of the magnetization at low temperatures. For the high-field limit the diamagnetic signal disappears and a positive moment is observed. Similar "reentry" phenomena have already been observed in other high- T_c systems.⁸ It is assumed that the magnetization (M_{FC}) in the superconducting region is composed of three sources: (i) the diamagnetic shielding moment; (ii) trapped flux; (iii) a paramagnetic contribution from Cu in the matrix. The inset of Fig. 4 summarizes the values of the volume Meissner frac-

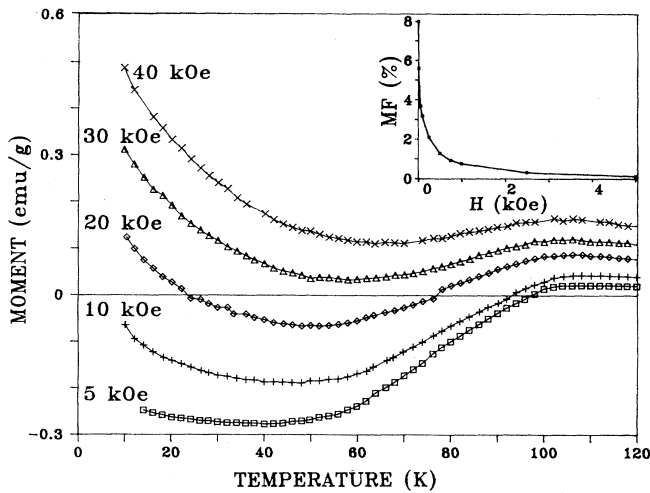


FIG. 4. FC magnetization curves at various magnetic fields. Note the upturn at 10 kOe and the positive values obtained at higher fields. The inset shows the Meissner fraction (MF) as a function of the applied field.

tion (MF) relative to $-1/4\pi$ obtained in this sample. It seems that the MF depends strongly on the applied field, and even at our lowest field (3.5 Oe) MF does not exceed 8% (see also Fig. 1). For $H=5$ kOe the MF is less than 0.2%. That means that in the high-field limit the trapped flux contribution is comparable to the diamagnetic shielding signal and they virtually cancel each other. Thus, it is obvious that in this range the paramagnetic contribution dominates, so that the total susceptibility is positive. The field dependence of the MF has been observed in other systems including single crystals of Y-Ba-Cu-O, where it is naturally explained in terms of the superconducting-glass model⁵ as well as in the framework of the conventional trapped flux picture.^{9,14}

C. Irreversibility line

In Figs. 1 and 3 the magnetic irreversibility which characterizes all type-II superconductors is shown. Above a field-dependent temperature T_{irr} , the ZFC and FC curves coincide, exhibiting the reversible region. The field dependence of T_{irr} is shown in the form of a field temperature phase diagram in Fig. 5. From the linearity of $\log_{10}[T_{irr}(0) - T_{irr}(H)]$ vs $\log_{10}H$ plot (inset of Fig. 5) we obtain a slope of 0.33 ± 0.02 . The fact that T_{irr} scales with the applied field as $H^{1/3}$ stands in contrast to other high- T_c superconductors,⁵⁻⁷ but the overall qualitative picture is quite similar.

Note, however, that the irreversibility line is shifted to relatively low temperatures in quite moderate fields. In this respect it differs from the Y-Ba-Cu-O system and resembles more the Bi-Sr-Ca-Cu-O results.¹⁵ There is a strong correlation between the exact temperature field dependence of the irreversibility line and the fact the MF is much smaller in this system. According to the picture proposed recently in the framework of the trapped flux model,¹⁴ the MF at low temperatures reflects the amount

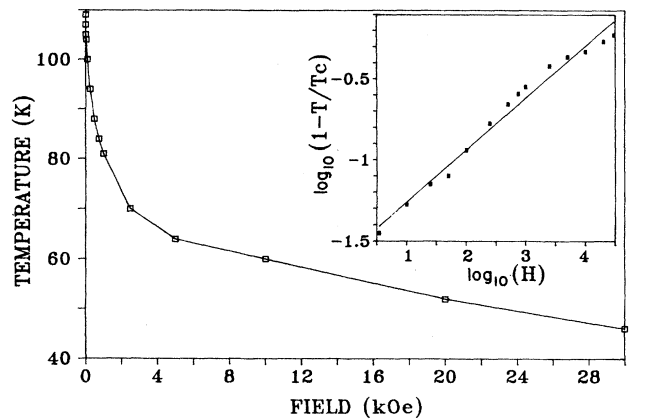


FIG. 5. The irreversible temperature T_{irr} as a function of the applied field. The inset shows the linear fitting to the \log_{10} - \log_{10} plot.

of flux which is trapped at the irreversibility line during the cooling process. This value might be calculated by using the Abrikosov equations, and it is quite obvious that more flux will be trapped if trapping occurs at lower temperatures.

D. Magnetization curves

Typical magnetization behavior at a constant temperature with the variation of the applied field is shown in Fig. 6 for 70 K. The procedure for getting this curve starts with ZFC of the sample to 70 K. Then the magnetization is recorded, while the field is increased up to 30 kOe and decreased to zero. It is obvious that above 5 kOe, in the reversible limit, both curves coincide while below this field the system enters the irreversible range. At 70 K this field matches the value obtained from the irreversibility line of the temperature-field phase diagram shown in Fig. 5. It implies that the isothermal field dependence of the magnetization curves provides us with an alternative method for obtaining the irreversibility line shown in Fig. 5. From M_{rem} obtained at $H=0$, the critical current of 4.5×10^4 A/cm² is obtained using the Bean relation $J_c = 30M_{rem}/r$

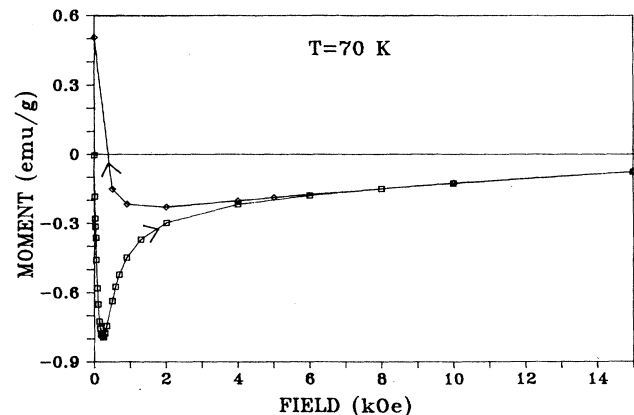


FIG. 6. Magnetic hysteresis curve at 70 K.

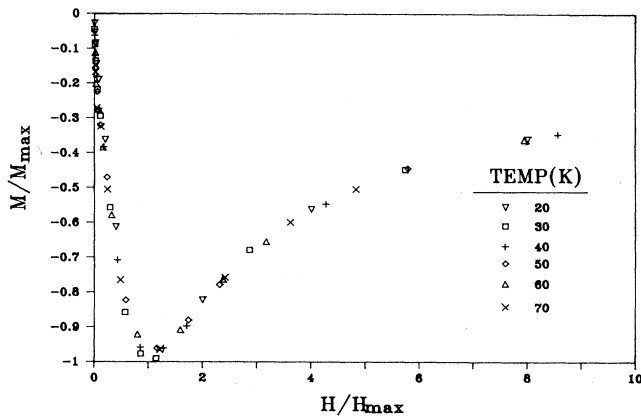


FIG. 7. Scaling of several magnetic curves at different temperatures (see text).

where $r = 10^{-3}$ cm is the average radius of a grain; the density is 3 g/cm^3 . J_c has an error of 20% due to the uncertainty of r .

Qualitatively, very similar curves to Fig. 6 are obtained at various temperatures, allowing us to scale all the magnetization curves using a simple procedure. We scale the field axis with H_{max} , the field for which M reaches its maximum value M_{max} ; similarly, we scale the M axis with M_{max} . The result of this scaling for several temperatures is exhibited in Fig. 7. Perfect scaling is obtained for fields and temperatures in the irreversible regions. Clear deviations from scaling are observed for fields and temperatures in the reversible range above the irreversibility line of Fig. 5. A complete description of this phenomenon will be published elsewhere.

E. Nonlinear magnetization above T_c

The temperature dependence of the normal-state magnetic susceptibility (M/H) for various fields is shown in Fig. 8. It is apparent from this figure that the magnetization does not vary linearly with H . The field dependence of the susceptibility at 170 K is given in the inset. The nonlinear behavior exists up to 40 kOe, the highest field used. M/H depends strongly on temperature in contrast to that of single-phase Y-Ba-Cu-O.¹⁶ Each of the curves in Fig. 8 can be fitted by a Curie-Weiss law plus a constant term, i.e., $M/H(T) = \chi_0 + C/(T - \Theta)$. For example, for $H = 1$ and 2.5 kOe, $\chi_0 = 2.3 \times 10^{-4}$ and 4.7×10^{-5} emu/mole, $C = 0.59$ and 0.63 emu/mole, and $\Theta = 11$ and -16 K, respectively. In general, χ_0 depends strongly on the applied field. It decreases by more than an order of

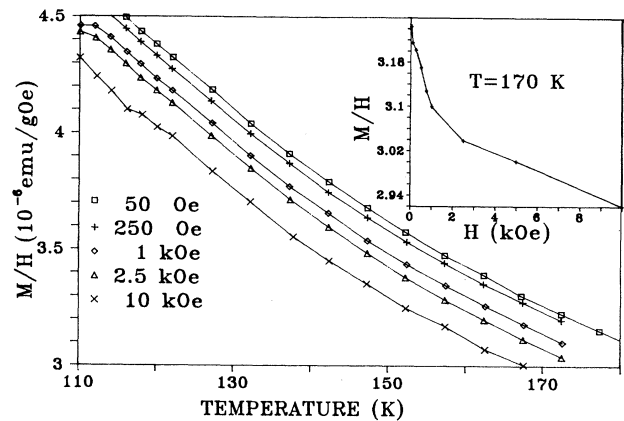


FIG. 8. Temperature dependence of magnetic susceptibility measured at various fields above T_c . In the inset: The variation of the susceptibility with the applied field is shown.

magnitude over the magnetic-field regime of the present study, while the Curie constant increases slightly with field. Similar field effects were also observed in Y-Ba-Cu-O.⁸ From the above values of the Curie constants we derive $P_{\text{eff}} = 1.26 \mu_B$ (Cu atom) which corresponds to a fraction of 73% spin- $\frac{1}{2}$ local moments of the Cu^{2+} ions ($1.71 \mu_B$). It means that the Curie-Weiss contribution to the susceptibility is intrinsic to the (2:2:2:3) single phase, and does not arise from impurity phases, since such a large concentration of an impurity phase would be easily visible in the x-ray-diffraction pattern.

It would be edifying to discover the source of the nonlinear magnetization behavior exhibited in Fig. 8. The existence of ferromagnetic impurities is excluded for the following reasons: (i) The nonlinear behavior continues at least up to 40 kOe (not shown in Fig. 8) and to relatively high temperatures ~ 300 K. No existing ferromagnetic compound with such a high Curie temperature which is not saturated at low temperatures at 40 kOe. (ii) To the best of our knowledge, there is no compound containing some of all the elements that constitute the 2:2:2:3 phase which is ferromagnetically ordered at about 300 K. We may assume that as in La_2CuO_4 ,¹⁷ magnetic correlations in the CuO_2 layers persist in the compound well above T_c ; their nature is now being studied.

ACKNOWLEDGMENTS

This research is supported by the German-Israel Foundation for Scientific Research and Development Grant No. I-40-100.10/87.

¹S. S. Parkin, V. Y. Lee, E. M. Engler, A. I. Nazzal, T. C. Huang, G. Gorman, R. Savoy, and R. Beyers, *Phys. Rev. Lett.* **60**, 2539 (1988).

²S. S. Parkin, V. Y. Lee, A. I. Nazzal, R. Savoy, T. C. Huang, G. Gorman, and R. Beyers, *Phys. Rev.* **38**, 6531 (1988).

³W. Reith, P. Muller, C. Allgeier, R. Hoben, J. Heise, J. S. Shilling, and K. Andres, *Physica C* **156**, 319 (1988).

⁴M. M. Fang, J. E. Ostenson, J. K. Finmore, D. E. Farrell, and N. P. Bansal, *Phys. Rev. B* **39**, 222 (1989).

⁵K. A. Müller, M. Takashige, and J. G. Bednorz, *Phys. Rev.*

- Lett. **58**, 1143 (1987).
- ⁶Y. Yeshurun and A. P. Malozemoff, *Phys. Rev. Lett.* **60**, 2202 (1988).
- ⁷I. Felner, Y. Wolfus, G. Hilscher, and N. Pillmayr, *Phys. Rev. B* **39**, 225 (1989).
- ⁸Y. Yeshurun, I. Felner, and H. Sompolinsky, *Phys. Rev. B* **36**, 840 (1987).
- ⁹L. Krusin-Elbaum, A. P. Malozemoff, and Y. Yeshurun, *Mater. Res. Soc. Symp. Proc.* **99**, 221 (1988).
- ¹⁰D. S. Ginely, B. Morosin, R. J. Boughman, E. L. Venturini, J. F. Schirber, and J. F. Kwak, *J. Cryst. Growth* (to be published).
- ¹¹L. Krusin-Elbaum, A. P. Malozemoff, Y. Yeshurun, and D. C. Cronemeyer (unpublished).
- ¹²S. Senoussi, M. Oussena, M. Ribault, and G. Collins, *Phys. Rev. B* **36**, 4003 (1987); S. Senoussi, M. Oussena, and S. Hadjoudj, *J. Appl. Phys.* **63**, 4176 (1988).
- ¹³C. P. Bean, *Phys. Rev. Lett.* **8**, 200 (1962).
- ¹⁴L. Krusin-Elbaum, A. P. Malozemoff, Y. Yeshurun, D. C. Cronemeyer, and F. Holtzberg, *Physica C* **153-155**, 1469 (1988).
- ¹⁵Y. Yeshurun, A. P. Malozemoff, T. K. Worthington, R. M. Yandrofski, L. Krusin-Elbaum, F. H. Holtzberg, T. R. Dingen, and G. V. Chandrasekhan, *Cryogenics* (to be published).
- ¹⁶S. W. Cheong, S. E. Brown, Z. Fisk, R. S. Kwok, J. D. Thompson, E. Zirngi, G. Gruner, D. E. Peterson, G. L. Wells, R. R. Schwarz, and J. B. Cooper, *Phys. Rev. B* **36**, 3913 (1987).
- ¹⁷M. A. Kastner, R. J. Bireneau, T. R. Thurston, P. J. Picone, H. P. Jenssen, D. R. Gable, M. Sata, K. Fukuda, S. Shamoto, Y. Endoh, K. Yamada, and G. Shirane, *Phys. Rev. B* **38**, 6636 (1988).